# REPORT No. 360

## PRESSURE DISTRIBUTION OVER A SYMMETRICAL AIRFOIL SECTION WITH TRAILING EDGE FLAP

By EASTMAN N. JACOBS and ROBERT M. PINKERTON
Langley Memorial Aeronautical Laboratory

# REPORT No. 360

## PRESSURE DISTRIBUTION OVER A SYMMETRICAL AIRFOIL SECTION WITH TRAILING EDGE FLAP

By Eastman N. Jacobs and Robert M. Pinkerton

SUMMARY

*Measurements were made in the Variable Density Wind Tunnel of the National Advisory Committee for Aeronautics to determine the distribution of pressure over one section of an R. A. F. 30 (symmetrical) airfoil with trailing edge flaps. In order to study the effect of scale, measurements were made with air densities of approximately 1 and 20 atmospheres.*

*Isometric diagrams of pressure distribution are given to show the effect of change in incidence, flap displacement, and scale upon the distribution. Plots of normal force coefficient versus angle of attack for different flap displacements are given to show the effect of a displaced flap. Finally, plots are given of both the experimental and theoretical characteristic coefficients versus flap angle, in order to provide a comparison with the theory. It is concluded that for small flap displacements the agreement for the pitching and hinge moments is such that it warrants the use of the theoretical parameters. However, the agreement for the lift is not as good, particularly for the smaller flaps. In an appendix, an example is given of the calculation of the load and moments on an airfoil with hinged flap from these parameters.*

### INTRODUCTION

Since a lifting surface with a trailing edge flap forms a part of the control system of practically every airplane, a study of such a surface is of particular importance. Some few tests have been made on airfoils having trailing edge flaps and among these is a force test in the Variable Density Wind Tunnel on an N. A. C. A–M6 airfoil. (Reference 4.) However, it is desirable to reduce the more general problem, first to one of determining the effect of a flap on the air forces acting at one section of a simple symmetrical airfoil. This report deals with an experimental investigation of this problem, the air forces being determined by measuring directly the pressures at points along one section of an R. A. F. 30 airfoil with flap.

This investigation is a part of a general investigation of the distribution of pressure over airfoils in the Variable Density Wind Tunnel at the Langley Memorial Aeronautical Laboratory. The purpose of the larger program is to study scale effect, and this part in particular, to study the effect of a flap. In keeping with the tendency toward smaller flaps a 10 per cent chord flap has been included and it would seem desirable that even smaller flaps be included in future investigations.

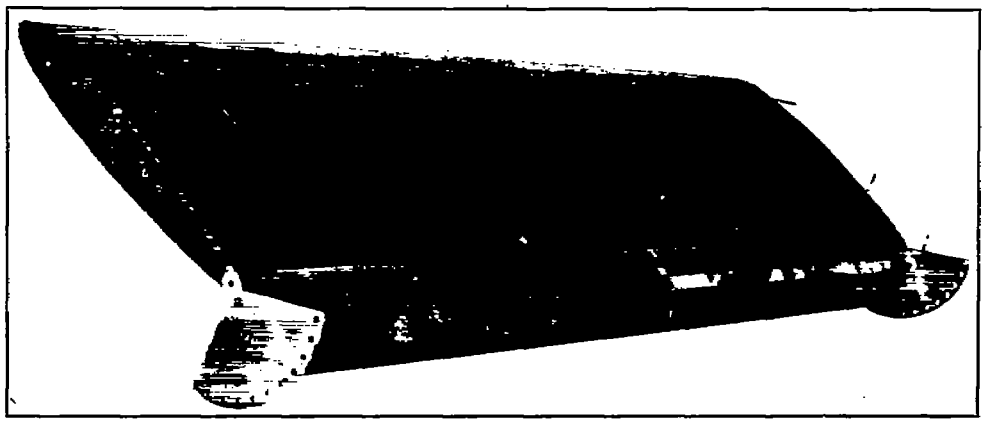

Figure 1.—Model R. A. F. 30 airfoil with trailing edge flap

### APPARATUS AND TESTS

A diagrammatic sketch of the redesigned Variable Density Wind Tunnel of the National Advisory Committee for Aeronautics and a description of the pressure distribution apparatus are given in Reference 2. A manually operated multiple-tube alcohol manometer was used to measure the pressure on the wing in the 1-atmosphere tests, but for the 20-atmosphere tests it was necessary to use an automatic photorecording manometer. A similar instrument is described in Reference 10.

The ordinates of the symmetrical R. A. F. 30 airfoil were taken from Reference 3 and are given in Figure 2. The model, shown in Figure 1, had a 10-inch chord

and 72-inch span, allowing it to extend across the 60-inch open test section and into the dead air space on both sides. It was constructed of mahogany, except for metal flaps. The entire 15 orifices were located at one section in the center of the airfoil and over one surface, as shown in Figure 2. Due to the symmetry of the section it was only necessary to record pressures on one surface, the pressures on the other surface being obtained from a similar record made with equal, but opposite, angles of attack and flap displacement. (The angle of attack, $\alpha$, is the angle of attack of the forward part of the airfoil.) For example, the pressure distribution over the section with a flap angle, $\delta$, of $+40°$ and an angle of attack, $\alpha$, of $+9°$ is found as follows: The upper surface pressures are given by the test in which $\delta=40°$ and $\alpha=9°$, and the lower surface pressures by the test in which $\delta=-40°$ and $\alpha=-9°$.

Pressures were measured for 10 and 20 per cent chord flaps with flap settings 0°, ±10°, ±20°, ±30°, ±40°, and ±50°, positive flap angles indicating a downward displacement. The angle of attack, $\alpha$, was varied in 3° intervals from $-21°$ to $+21°$ for the 10 per cent chord flap and from $-28°$ 30′ to $+28°$ 30′ for the 20 per cent chord flap. The tests were made with air pressures in the tunnel of approximately 1 and 20 atmospheres, corresponding to Reynolds Numbers of approximately $0.356\times10^6$ and $6.70\times10^6$.

in neutral position. These diagrams were mechanically integrated to obtain the coefficients of normal force, pitching moment about a point one-quarter of the chord behind the leading edge, flap load, and hinge moment, the coefficients being defined by the following expressions:

$$C_{NF}=\frac{F}{qS}$$

$$C_M=\frac{M}{qSc}$$

$$C_{NF_f}=\frac{F_f}{qS_f}$$

$$C_h=\frac{M_h}{qS_f c_f}$$

where $F$ is the resultant pressure force normal to the chord, $M$ the corresponding moment about the quarter-chord point, $F_f$ the resultant pressure force on the flap normal to the chord of the flap, and $M_h$ the corresponding moment about the flap hinge. The subscript $f$ refers to the flap, the flap chord, $c_f$, being measured from the hinge.

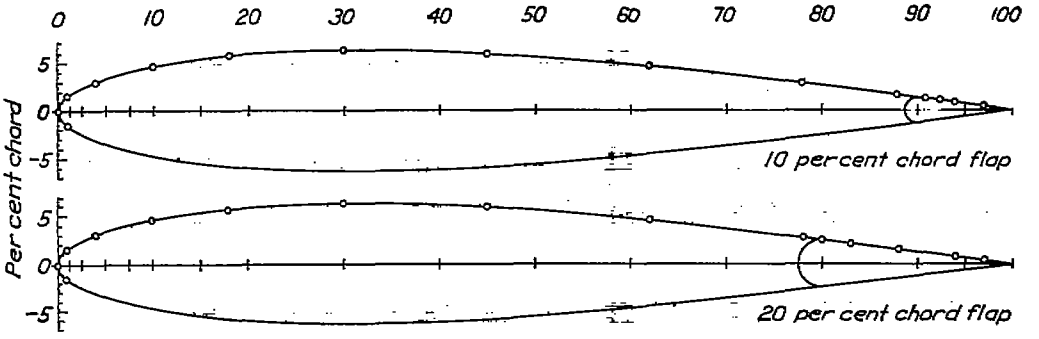


| % c'd | 0 | 1.25 | 2.5 | 5 | 7.5 | 10 | 15 | 20 | 30 | 40 | 50 | 60 | 70 | 80 | 90 | 95 | 100 |
|---|---|---|---|---|---|---|---|---|---|---|---|---|---|---|---|---|---|
| Up'r. | 0.00 | 1.80 | 2.48 | 3.46 | 4.15 | 4.68 | 5.44 | 5.94 | 6.32 | 6.20 | 5.66 | 4.78 | 3.70 | 2.50 | 1.30 | .70 | 0.00 |
| L'w'r | 0.00 | -1.80 | -2.48 | -3.46 | -4.15 | -4.68 | -5.44 | -5.94 | -6.32 | -6.20 | -5.66 | -4.78 | -3.70 | -2.50 | -1.30 | -.70 | 0.00 |

FIGURE 2.—R. A. F. 30 sections showing pressure orifice locations for 10 and 20 per cent chord flaps

## RESULTS

The results of this investigation are given in the form of diagrams and curves in Figures 3 to 23, inclusive. The diagrams showing the distribution of pressure were obtained by plotting the ratio $p/q$, the local pressure $p$ at each orifice, measured with respect to the pressure in the dead air space about the jet, divided by the dynamic pressure $q$, against the location of the orifice along the chord.

It should be noted that in the construction of the diagrams, the chord of the wing is taken the same in all diagrams; namely, the chord of the wing with flap

The system of plotting the pressures on the flap introduces a small error in the values of $C_{NF}$ and $C_M$ but does not affect the values of $C_{NF_f}$ and $C_h$. A better approximation would be to assume that the pressures act normal to the broken line representing the mean camber line of the section. The corrected coefficients of normal force and pitching moment would then be:

$$C_{NF}\ (\text{cor.})=C_{NF}-E\ (1-\cos\delta)\ C_{NF_f}.$$

$$C_M\ (\text{cor.})=C_M+E\ (1-\cos\delta)\ (.75-E)\ C_{NF_f}.$$

Inasmuch as the theory is based on an assumption which gives accurate values only for small flap angles, the above corrections have no bearing on the comparison between theory and experiment.

Isometric diagrams showing the distribution of pressure under typical conditions are given in Figures 3 to 11. In Figures 3 to 8 both the low and high Reynolds Number data, for the airfoil with 20 per cent chord flap, have been plotted together. In

Figures 9 to 11 corresponding low Reynolds Number data, for the airfoil with 10 per cent chord flap, are plotted, the high Reynolds Number data being omitted, since as a result of difficulties with the equipment, they were not considered sufficiently reliable to present.

The integrated data are presented in Figures 12 to 23 in which the integrated coefficients are plotted against angle of attack. In addition to these and more pertinent to this investigation the coefficients of normal force, pitching moment, and hinge moment are plotted against flap displacement in Figures 25 to 32. These figures were obtained by cross-fairing the original plots.

In comparing the curves for scale effect it must be remembered that the high scale tests were less accurate than the low scale tests for several reasons. The model mounting lacked sufficient rigidity to maintain accurately its angle calibration when subjected to the large forces encountered during a high scale run. The width of the lines on the photomanometer records was of the order of that which would be produced by pressure pulsations of ±10 per cent of the dynamic pressure, and the manometer cells were subject to errors in their respective calibrations. Further recent studies of the effect of temperature on the calibrations of the manometer cells have shown that errors in the individual pressures as high as 10 per cent may have been introduced in this way. A part of the difference between the high and the low scale results of these tests may, therefore, be due to inaccuracies of measurement.

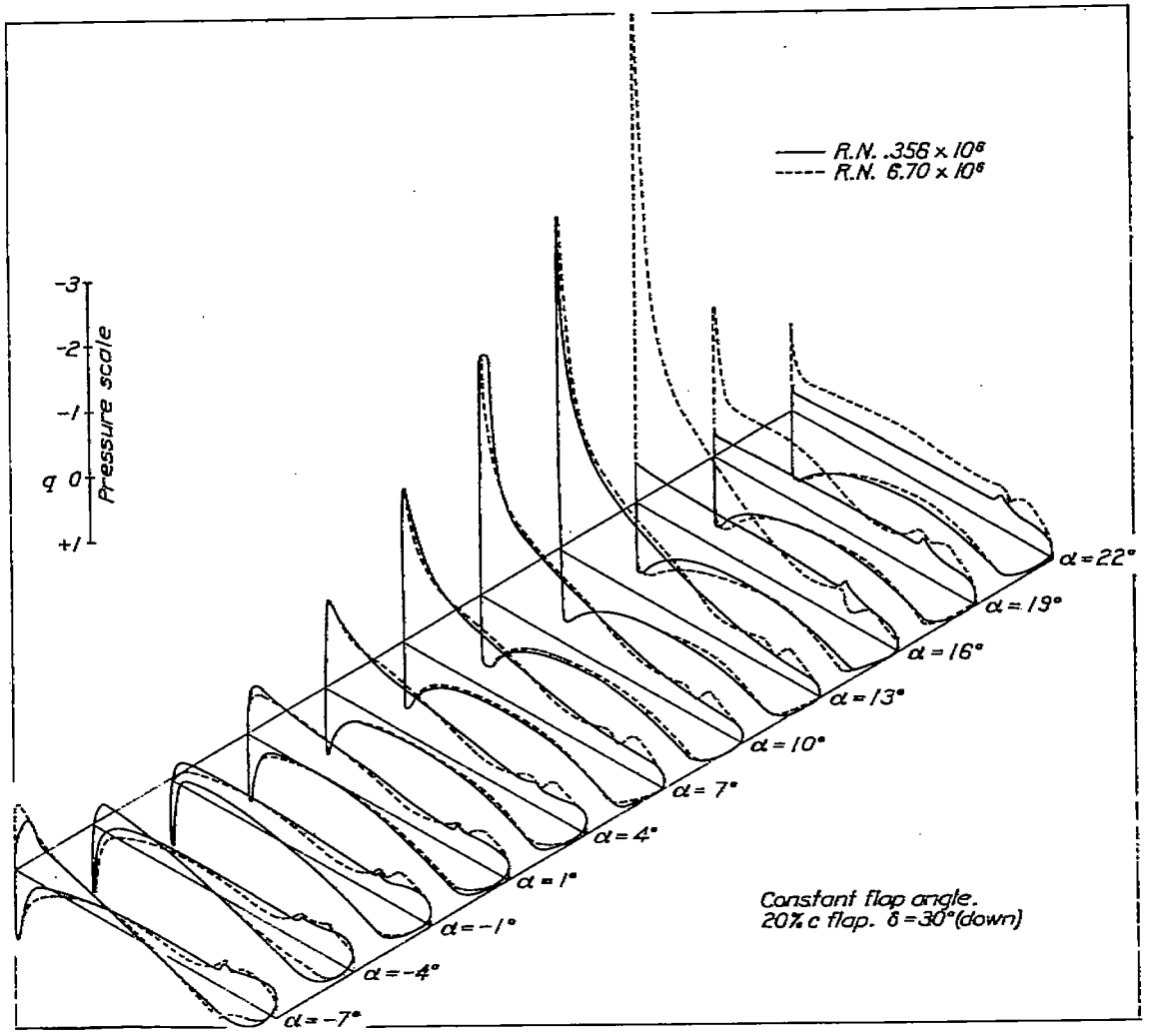


FIGURE 8

## DISCUSSION

**Distribution of pressure:**

The change in the distribution of pressure over the R.A.F. 30 airfoil, resulting from an increase in dynamic scale or Reynolds Number can be observed in Figures 3 to 8. In accordance with previous observations, the effect is confined largely to the distribution in the region of the burble. The burble is very definitely delayed by an increase in scale, and the negative pressures attained in the high-scale tests exceed the negative pressures attained in the low-scale tests. Figure 7 shows the distribution in the region of

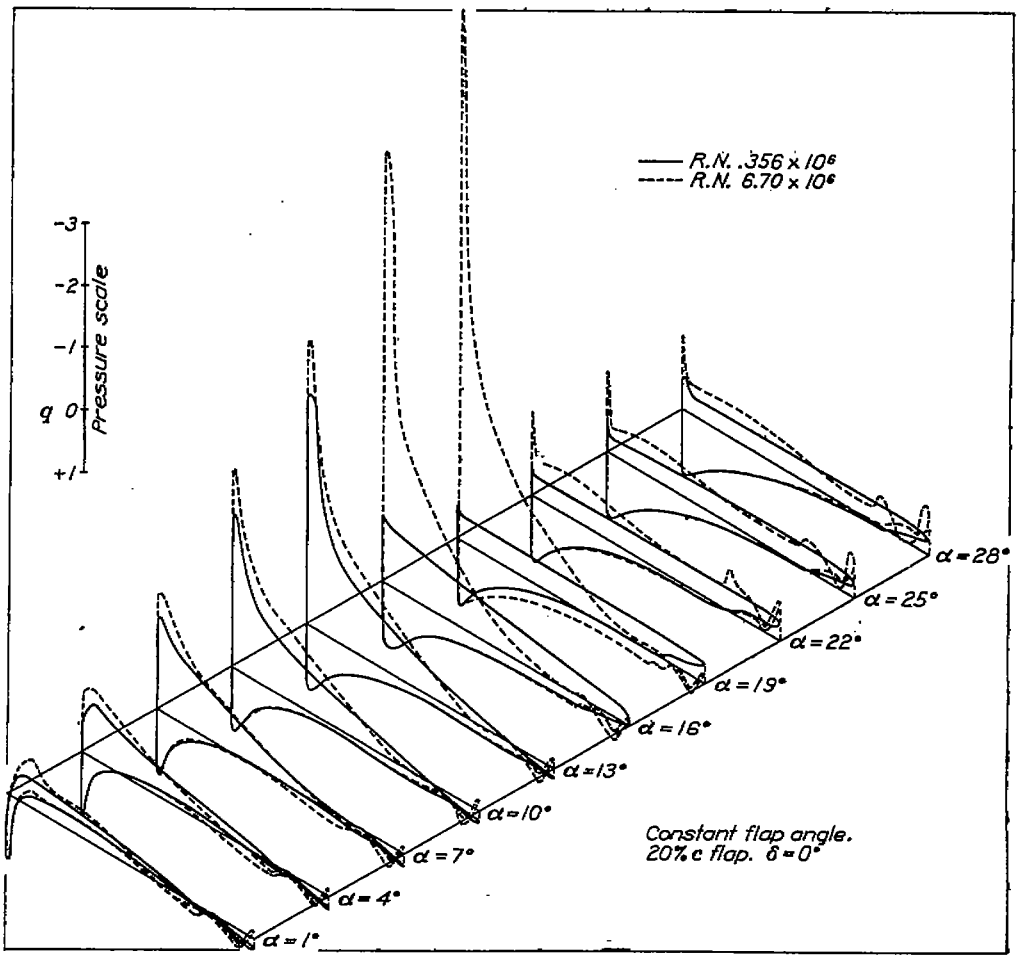


FIGURE 4

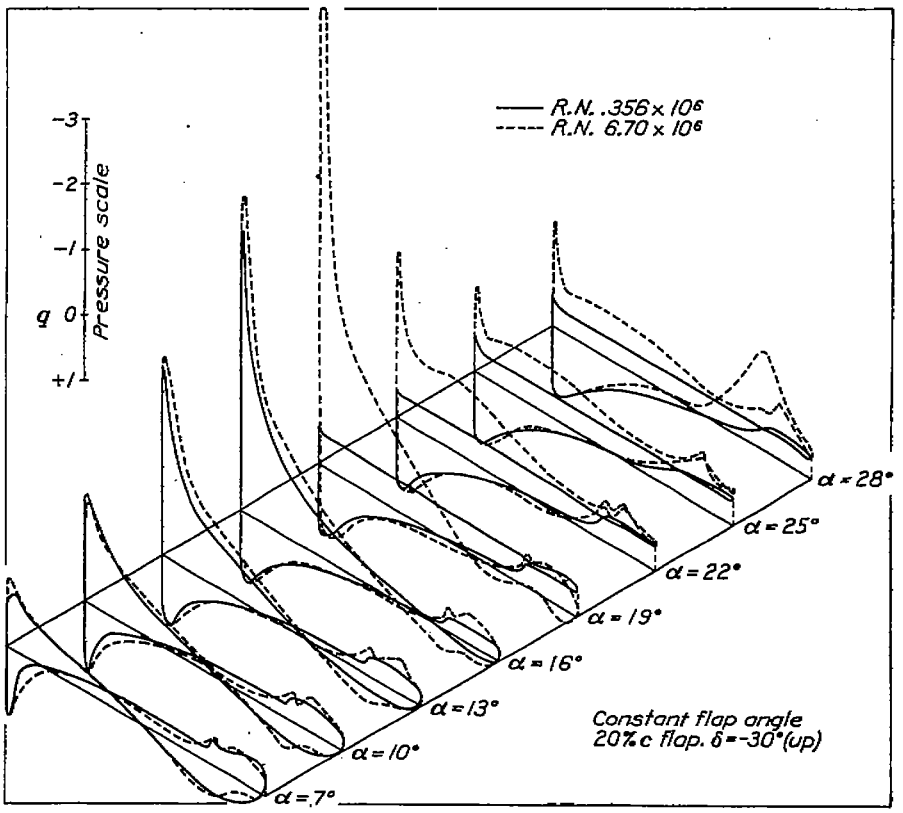


FIGURE 5

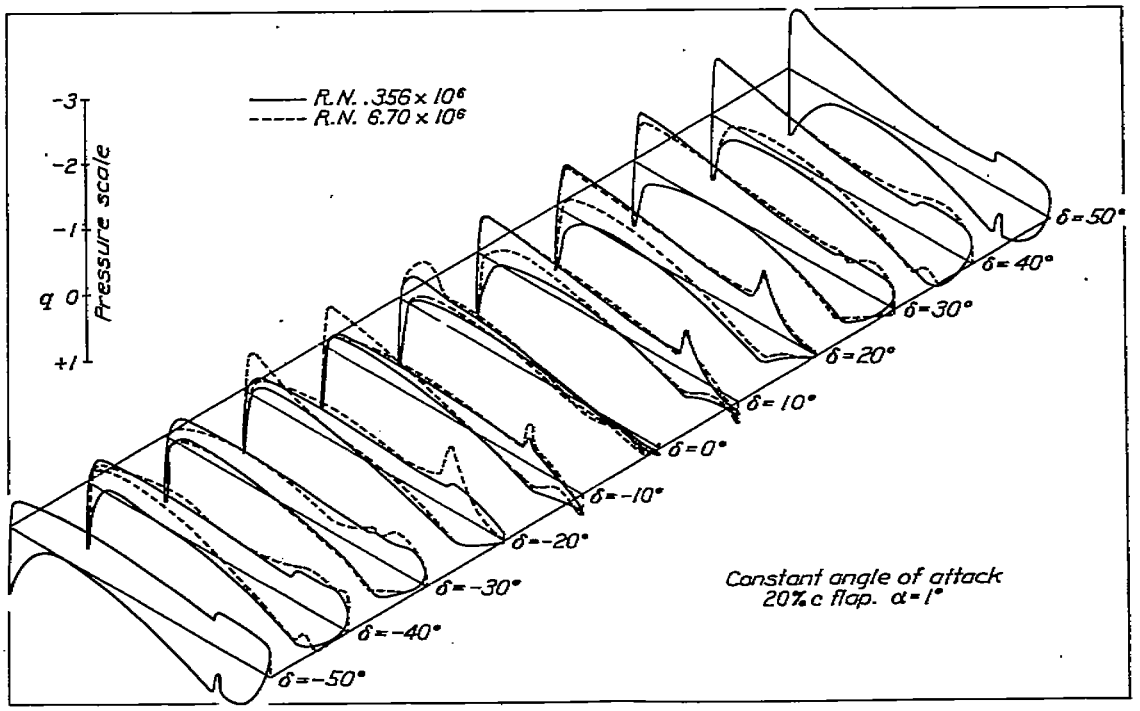


FIGURE 6

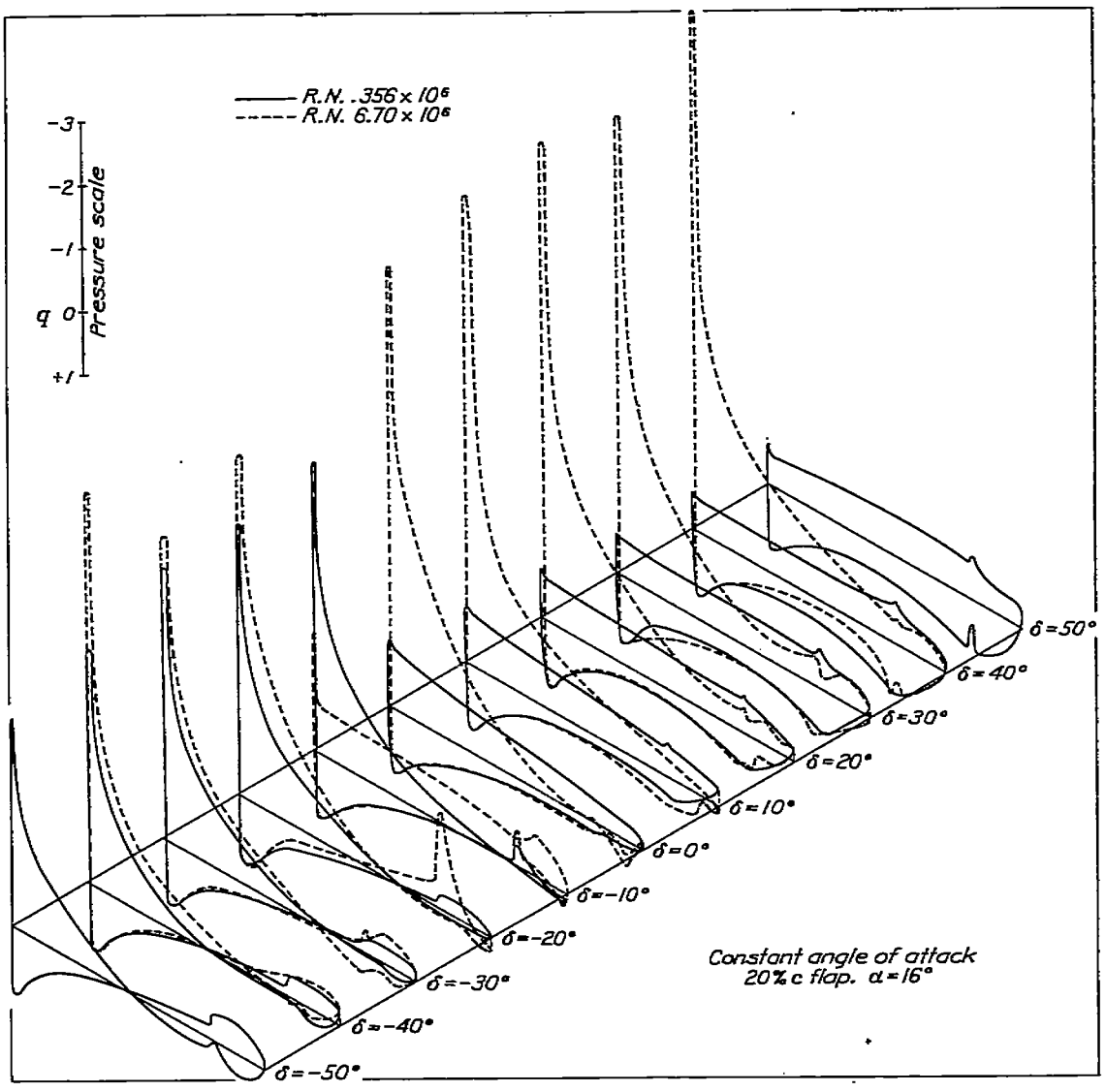


FIGURE 7

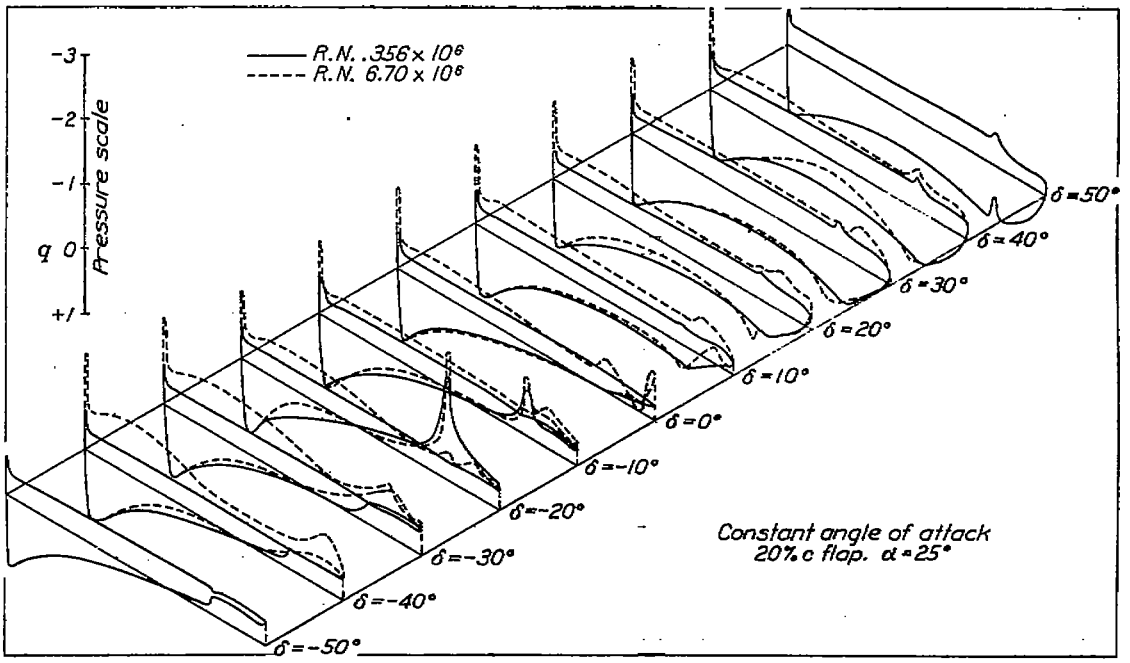


FIGURE 8

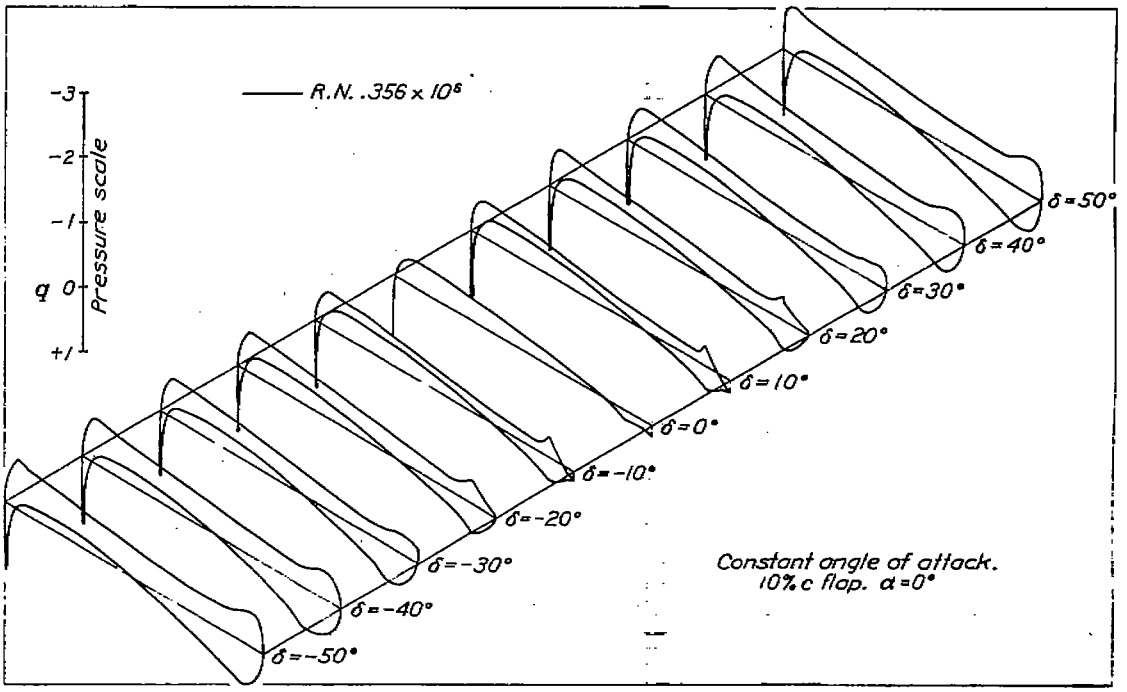


FIGURE 9

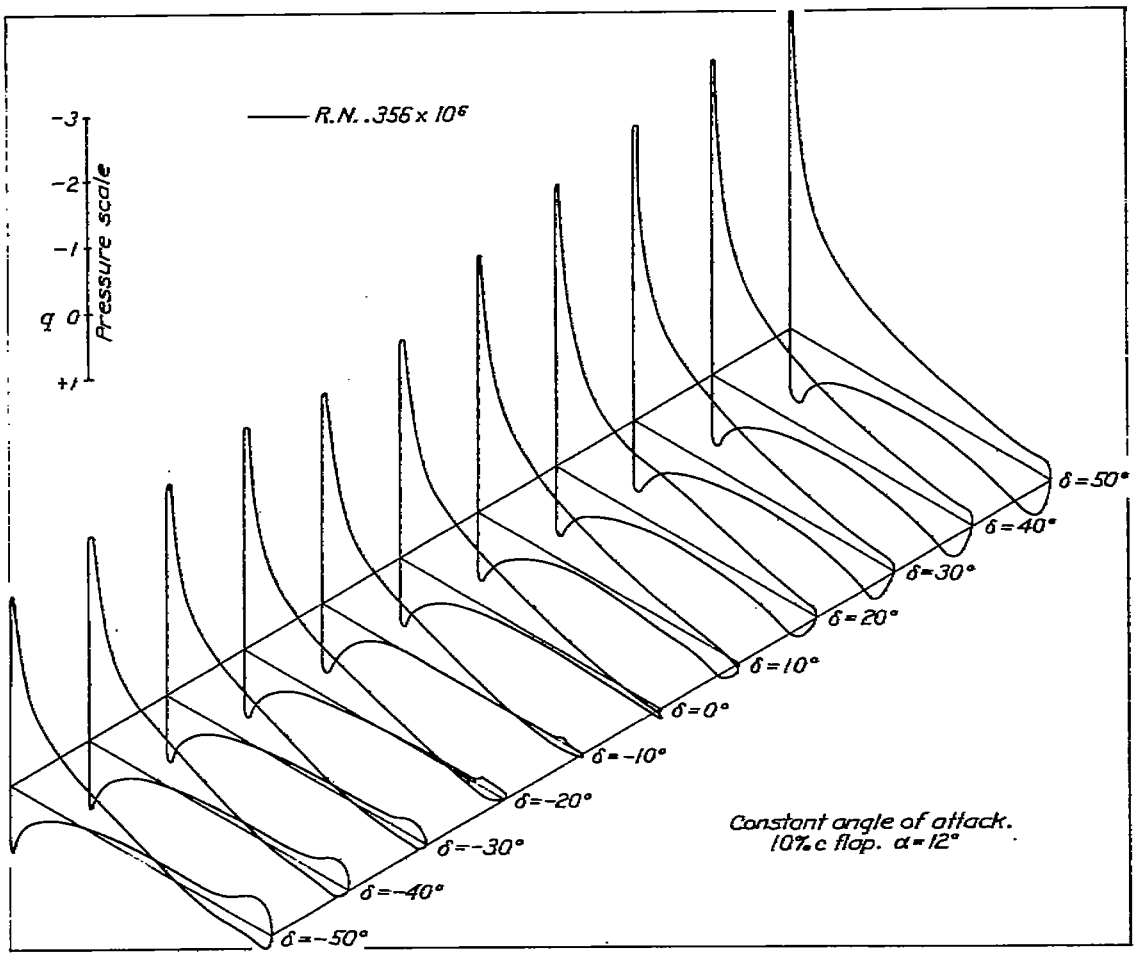


FIGURE 10

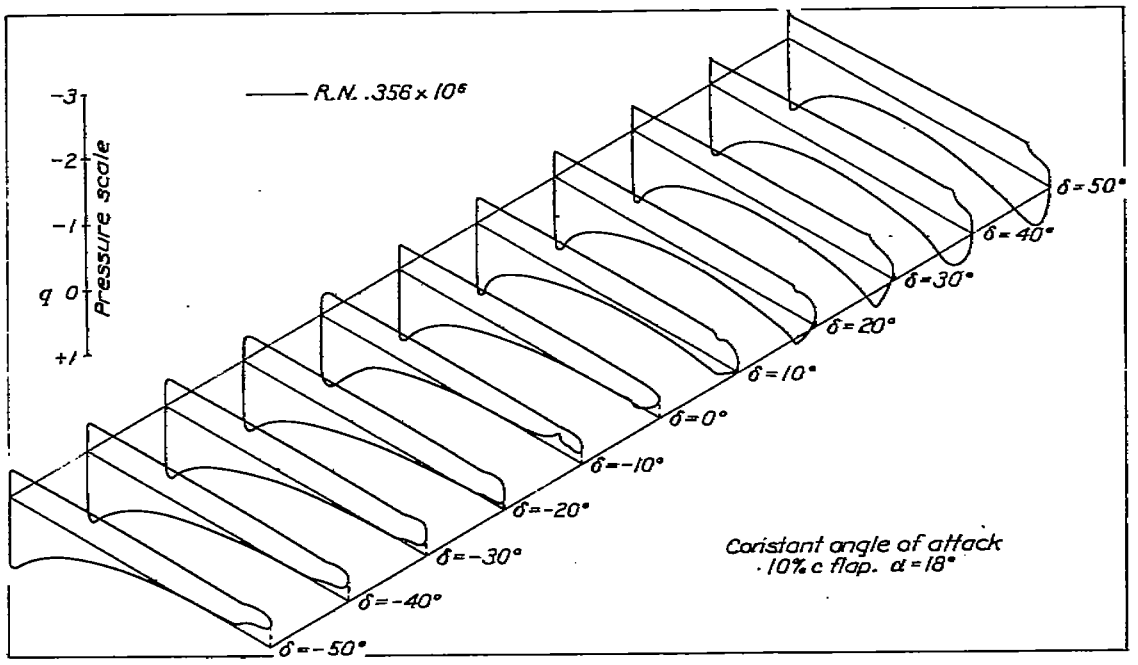


FIGURE 11

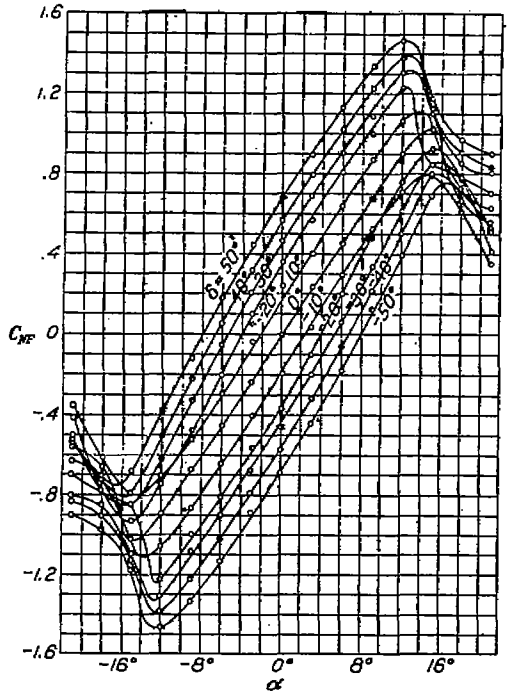


FIGURE 12.—Normal force coefficient versus angle of attack for different flap angles; 10 per cent c flap. Reynolds Number 0.356×10⁶

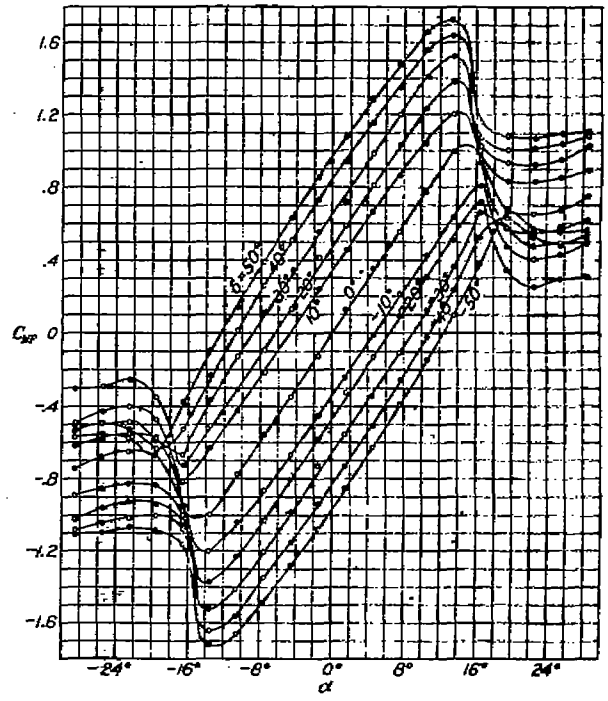


FIGURE 13.—Normal force coefficient versus angle of attack for different flap angles; 20 per cent c flap. Reynolds Number 0.356×10⁶

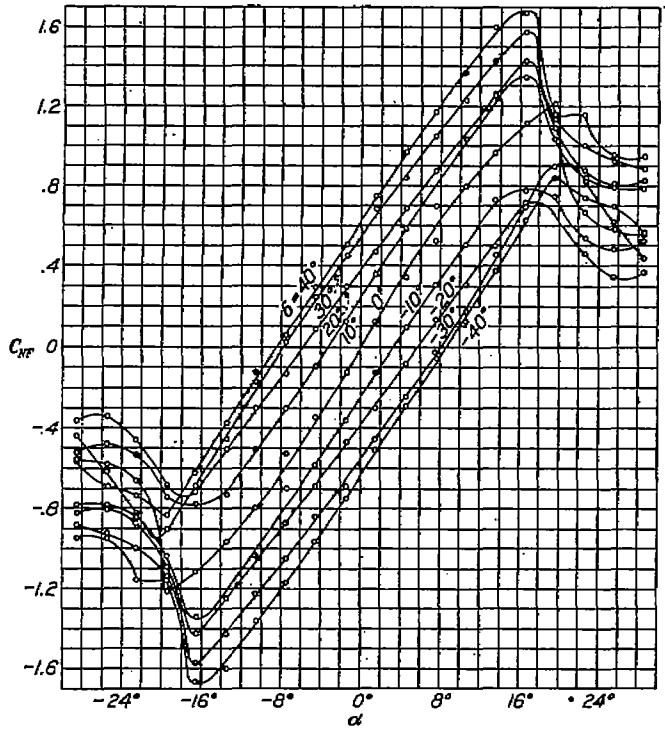


FIGURE 14.—Normal force coefficient versus angle of attack for different flap angles; 20 per cent c flap. Reynolds Number 6.70×10⁶

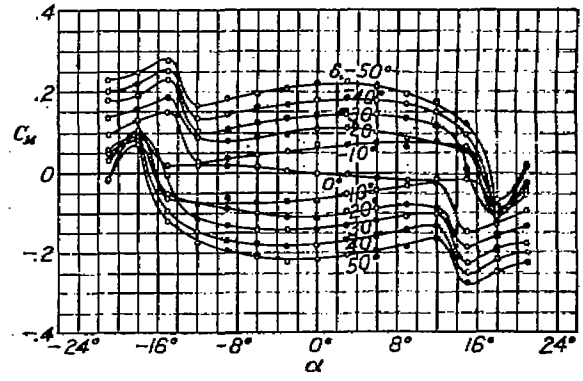


FIGURE 15.—Pitching moment coefficient versus angle of attack for different flap angles; 10 per cent c flap. Reynolds Number 0.356×10⁶

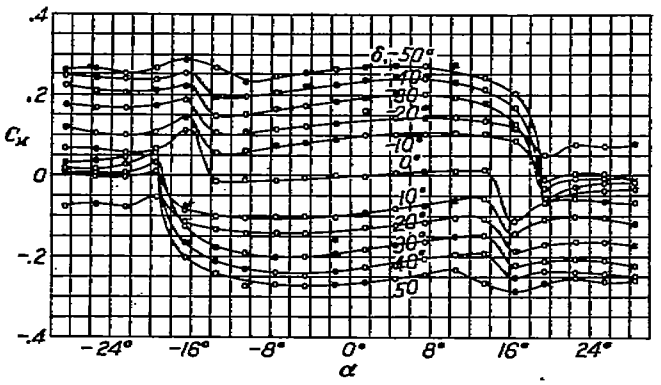


FIGURE 16.—Pitching moment coefficient versus angle of attack for different flap angles; 20 per cent c flap. Reynolds Number 0.356×10

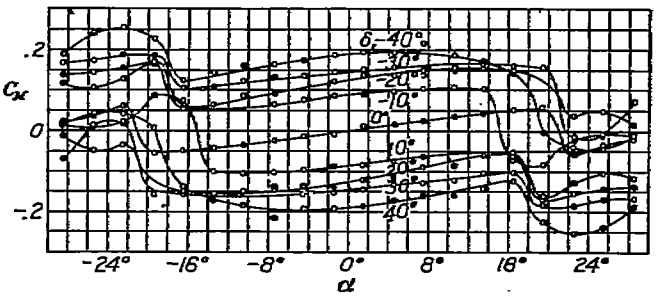


FIGURE 17.—Pitching moment coefficient versus angle of attack for different flap angles; 20 per cent c flap. Reynolds Number 6.70×10⁶

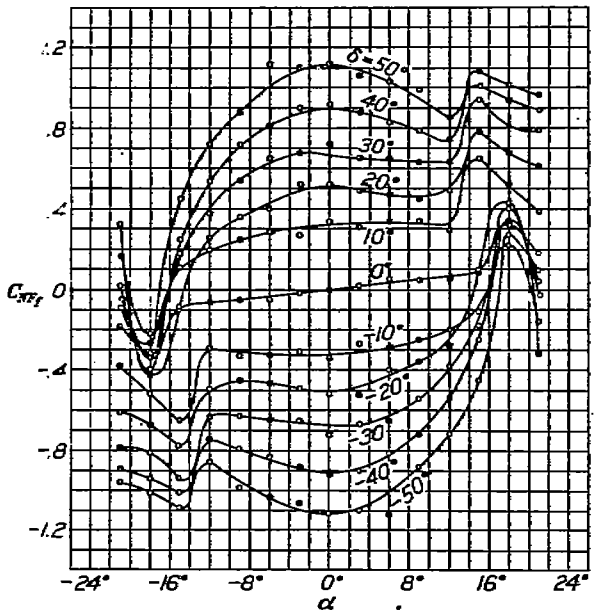


FIGURE 18.—Flap load coefficient versus angle of attack for different flap angles; 10 per cent c flap. Reynolds Number 0.356×10⁶

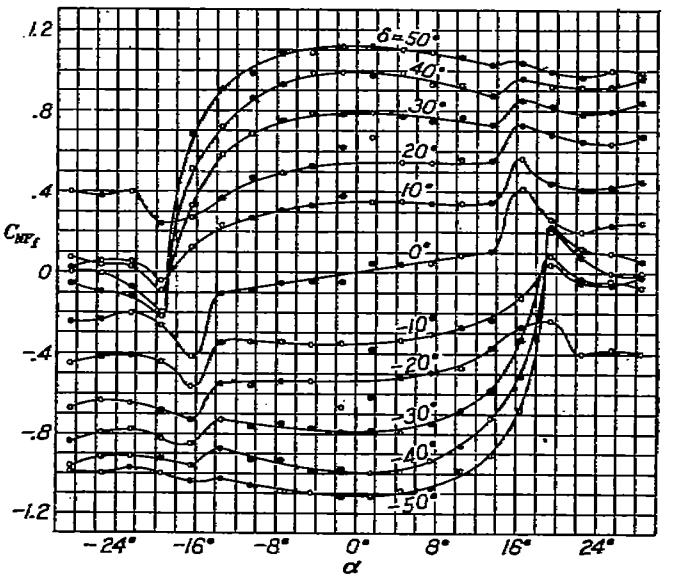


FIGURE 19.—Flap load coefficient versus angle of attack for different flap angles; 20 per cent c flap. Reynolds Number 0.356×10⁶

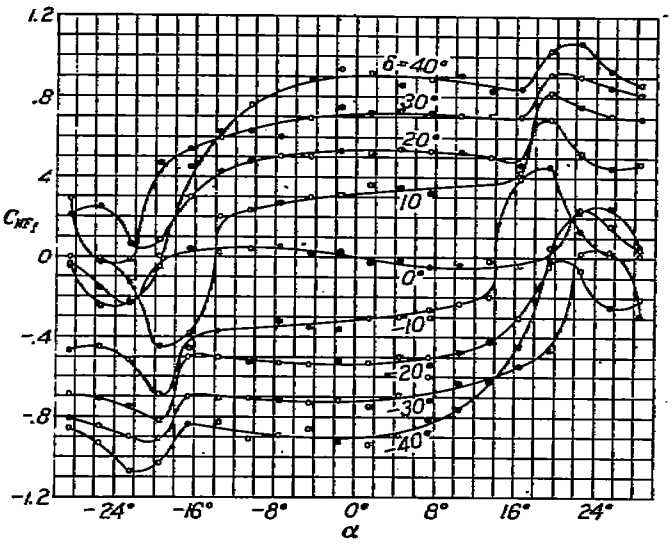


FIGURE 20.—Flap load coefficient versus angle of attack for different flap angles; 20 per cent c flap. Reynolds Number 6.70×10⁶

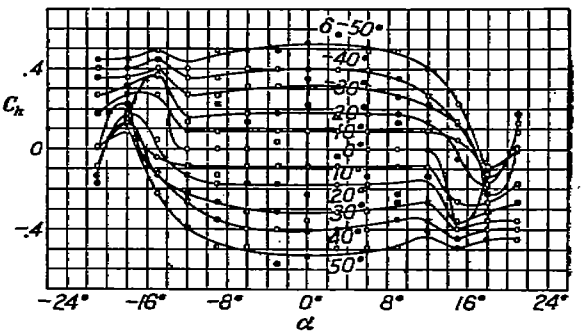


FIGURE 21.—Hinge moment coefficient versus angle of attack for different flap angles; 10 per cent c flap. Reynolds Number 0.356×10⁶

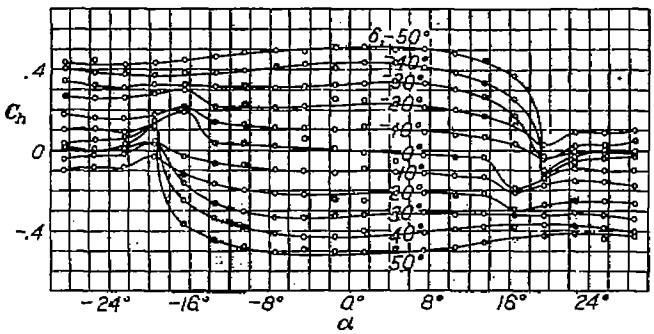


FIGURE 22.—Hinge moment coefficient versus angle of attack for different flap angles; 20 per cent c flap. Reynolds Number 0.356×10⁶

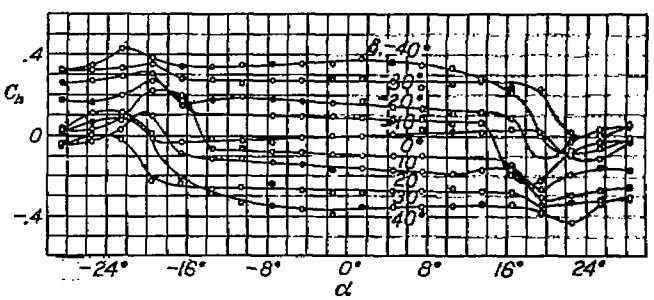


FIGURE 23.—Hinge moment coefficient versus angle of attack for different flap angles; 20 per cent c flap. Reynolds Number 6.70×10⁶

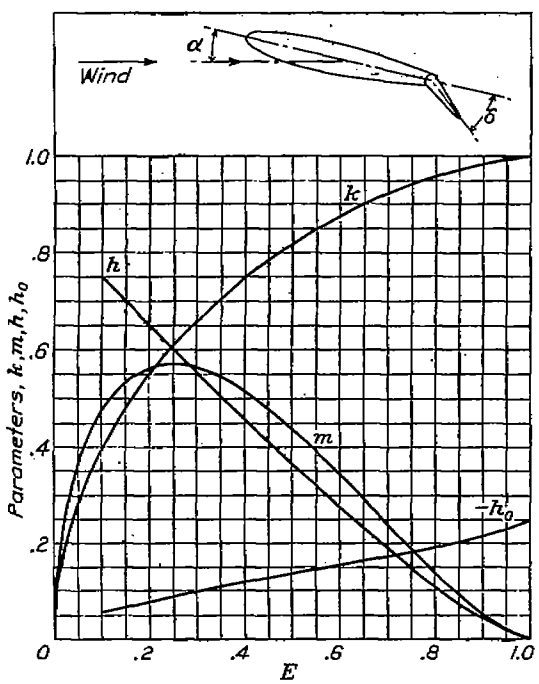


FIGURE 24.—Theoretical parameters (independent of aspect ratio)

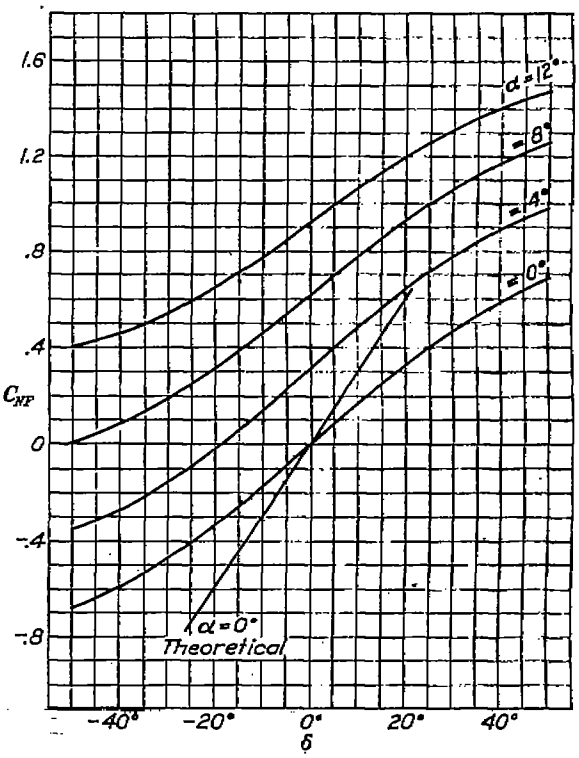


FIGURE 25.—Normal force coefficient versus flap angle at different angles of attack; 10 per cent c flap. Reynolds Number 0.356×10⁶

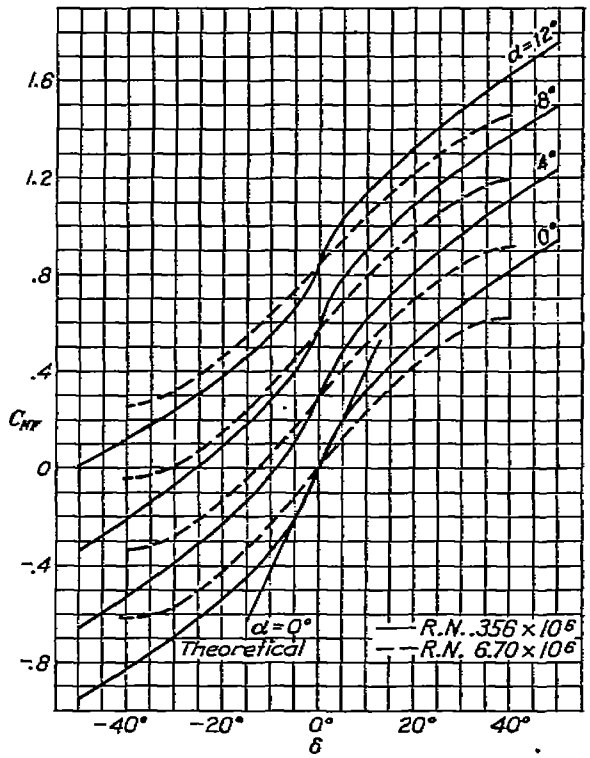


FIGURE 26.—Normal force coefficient versus flap angle at different angles of attack; 20 per cent c flap

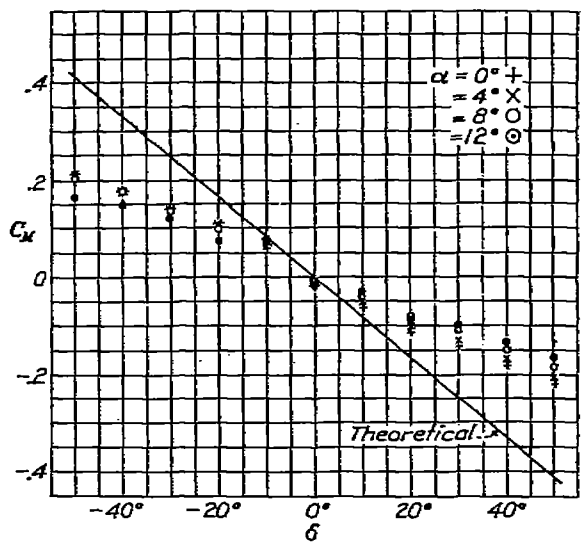


FIGURE 27.—Pitching moment coefficient versus flap angle at different angles of attack; 10 per cent c flap. Reynolds Number 0.356×10⁶

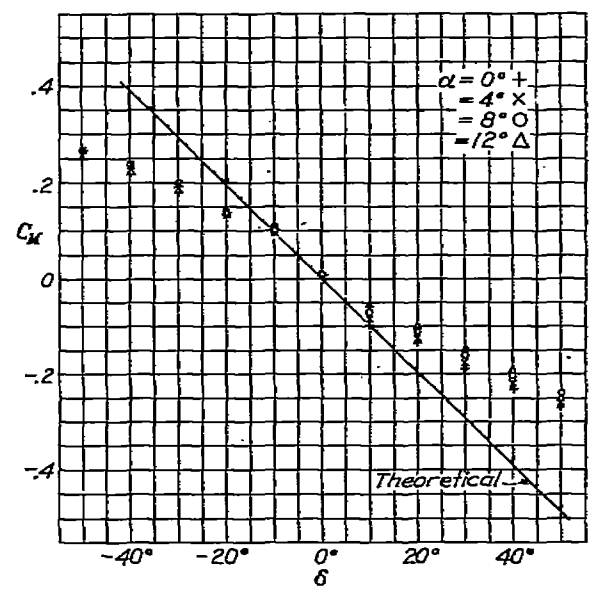


FIGURE 28.—Pitching moment coefficient versus flap angle at different angles of attack; 20 per cent c flap. Reynolds Number 0.356×10⁶

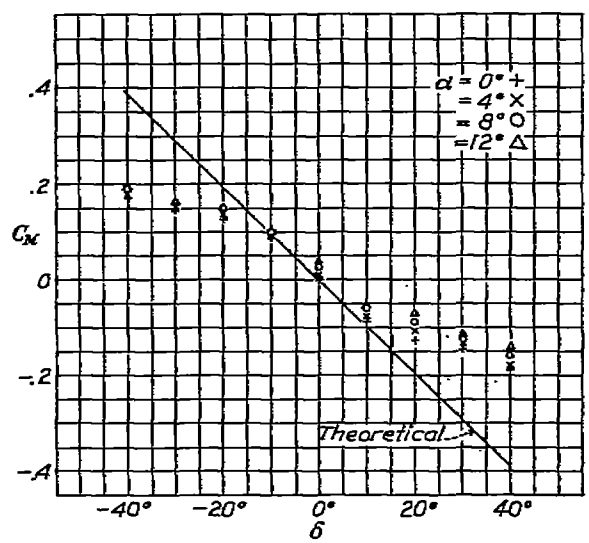


FIGURE 29.—Pitching moment coefficient versus flap angle at different angles of attack; 20 per cent c flap. Reynolds Number 6.70×10⁶

the burble through the entire range of flap displacements for the airfoil with 20 per cent chord flap.

When the forward part of the airfoil is maintained at a constant angle of attack and the flap is displaced, a series of pressure distribution diagrams showing the effect of displacing the flap is obtained. Such diagrams are given for angles of attack corresponding approximately to zero lift, maximum lift, and to lifts well beyond the stall in Figures 6 to 11. As the flap is displaced from the neutral position, while the angle of the forward part of the airfoil is maintained unchanged, a secondary burbling condition may be observed at the hinge in some of the diagrams. For instance, in Figures 6 to 8, particularly at $\delta = -20°$, there is, on the lower surface at the hinge, a noticeable negative pressure peak. These peaks, which are more pronounced at the higher Reynolds Number, disappear as the flap angle $\delta$ is increased, indicating burbling of the flow over the flap at angles greater than 20°.

**The effect of a flap:**

An airfoil having its trailing edge flap displaced becomes, in effect, a new airfoil having a different camber. If the flap is displaced downward, the camber becomes larger and the airfoil would be expected to have a larger negative angle of zero lift and a higher maximum lift. The lift curve below the burble region, however, would be expected to remain a straight line having approximately the same slope. Referring to Figures 12 to 14, it is seen that the effect of displacing the flap through small angles may be predicted in this way, but for larger flap angles there probably is a local burbling condition over the flap which causes the flap effect to become more complicated. For instance, as previously pointed out while considering the pressure distribution diagrams, there is apparently a change in flow over the 20 per cent chord flap when it is displaced upward to angles between 20° and 30°. At the higher Reynolds Number (fig. 14) the maximum normal force coefficient is higher at the larger negative flap angle and the normal force coefficient curve has an abnormally high slope. At higher negative flap angles the normal force curve slope remains high, but the maximum normal force falls off again. A similar effect, but occurring at smaller negative flap angles

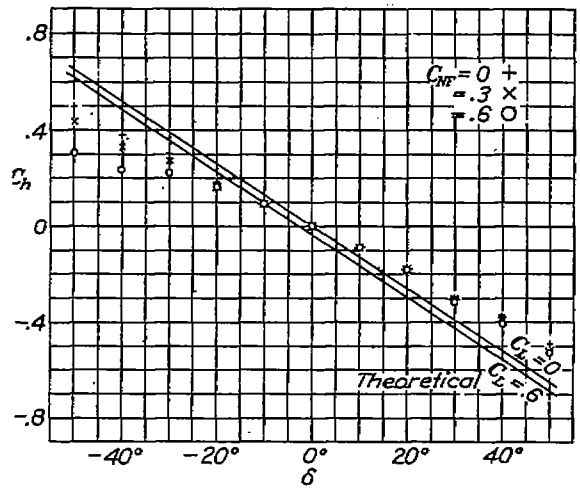


FIGURE 30.—Hinge moment coefficient versus flap angle at different values of $C_{NF}$; 10 per cent $c$ flap. Reynolds Number 0.356×10⁶

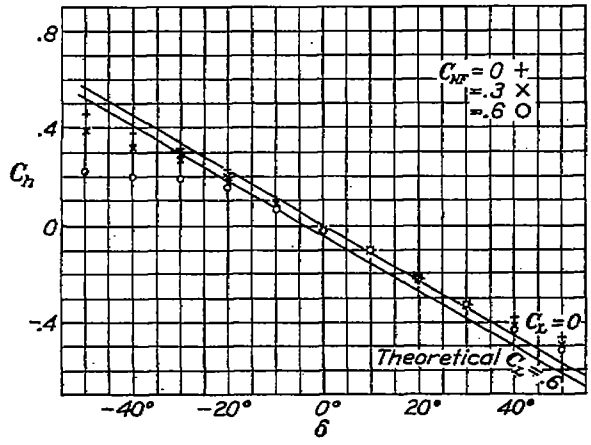


FIGURE 31.—Hinge moment coefficient versus flap angle at different values of $C_{NF}$; 20 per cent $c$ flap. Reynolds Number 0.356×10⁶

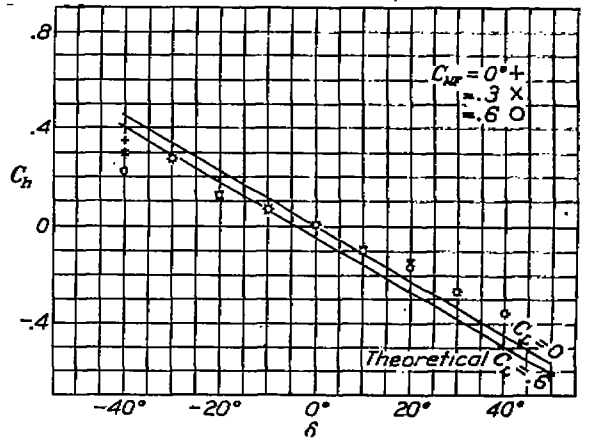


FIGURE 32.—Hinge moment coefficient versus flap angle at different values of $C_{NF}$; 20 per cent $c$ flap. Reynolds Number 6.70×10⁶

may be observed in the diagrams for the airfoil with 10 per cent chord flap.

Theory does not enable the prediction of the maximum lift coefficient of an airfoil with a flap, but it may be concluded from Figures 12 to 14 that displacing the flap downward to angles as large as 50° will produce a progressive increase in the maximum lift coefficient, and that the airfoil will burble at the same or a slightly lower angle of attack as the flap is displaced downward. The effect of increasing the scale is to increase the maximum normal force coefficient for all down-flap settings, the burble angle being approximately 3° higher at the high scale, but the change in maximum normal force coefficient as a result of displacing the flap is not as great at the larger Reynolds Numbers. In other words, the increase in maximum normal force coefficient with scale is greater for the small flap displacements. Values of maximum normal force coefficient for different flap angles are given in the table below.

TABLE I

| Flap angle | −50° | −40° | −30° | −20° | −10° | 0° | 10° | 20° | 30° | 40° | 50° |
|---|---|---|---|---|---|---|---|---|---|---|---|
| 10 per cent $c$ R. N. 0.356 × $10^6$ | 0.75 | 0.80 | 0.86 | 0.92 | 0.79 | 1.02 | 1.11 | 1.23 | 1.32 | 1.39 | 1.46 |
| 20 per cent $c$ R. N. 0.356 × $10^6$ | .67 | .63 | .66 | .72 | .81 | 1.02 | 1.21 | 1.38 | 1.52 | 1.64 | 1.72 |
| 20 per cent $c$ R. N. 6.70 × $10^6$ | | .83 | .92 | .72 | .78 | 1.21 | 1.35 | 1.42 | 1.57 | 1.68 | |

Before proceeding with the comparison of theory and experiment, it is necessary to consider the effect of aspect ratio and determine some means of taking this variable into account. Assuming that a change in the aspect ratio does not alter the angle of zero lift or the distribution of air forces over the airfoil at a particular value of the lift, expressions are derived containing parameters which are independent of the aspect ratio.

The shift of the angle of zero lift with flap displacement has been found theoretically by applying Munk's integrals to the broken line representing the mean camber line of the deformed section (References 4 and 5.) The theory indicates that this shift is proportional to the angular displacement of the flap for the small angles and may be represented as a fraction, $k$, of the flap displacement angle. For instance, if $k=0.5$, displacing the flap 10° will produce the same change in the lift as displacing the whole undeformed airfoil through an angle of 5°. The angle of attack measured from the angle of zero lift, for a symmetrical airfoil with a flap displaced through the angle $\delta$, is, therefore, $(\alpha+k\delta)$. Hence

$$C_L=a(\alpha+k\delta) \tag{1}$$

where $a$ is the slope of the lift curve corresponding to any particular aspect ratio under consideration and $k$ is independent of aspect ratio. Munk's integrals when applied to the broken line representing the median line of the section, give

$$k=\frac{\cos^{-1}(1-2E)+2\sqrt{E(1-E)}}{\pi} \tag{2}$$

where $E$ is the ratio of the flap chord to the total chord. This expression gives the same result as that given by Glauert (Reference 6). For convenience, the values of $k$, as calculated from the above expression, are plotted against $E$ in Figure 24.

Neglecting slight differences between the lift coefficient and the normal force coefficient, which for the conditions under consideration would not amount to more than about plus or minus 2 per cent, the experimental and theoretical values of $k$ may be compared by referring to the curves of normal force coefficient versus flap angle, $\delta$, for constant angles of attack, $\alpha$. Equation (1) indicates that theoretically these curves are straight lines having a slope of $a\,k$.

The value of "$a$" for this comparison has been obtained from the experimental curves. Taking a value for $a$ of 0.075 per degree (4.30 per radian) as a mean slope of the normal force coefficient curves, lines representing the theoretical curves have been drawn, together with the experimental curves in Figures 25 and 26. A comparison of the slopes of the lines in Figure 25 shows that for a 10 per cent chord flap only about 50 per cent of the theoretical effect of the flap on the normal force coefficient is attained. Increasing the flap size to 20 per cent of the chord (fig. 26) produces an increase in effectiveness as compared with the theoretical, particularly for small flap displacements. At the lower Reynolds Number when the 20 per cent chord flap is displaced 10°, about 80 per cent of the full theoretical effect is reached. Figure 26 shows that the high scale results do not agree as well with the theory. This might be expected, since previous work has shown that small irregularities such as hinges and hinge fairings produce a much larger disturbance at high scale than at low.

Further evidence of increased effectiveness of larger flaps as compared with the theory is found in Reference 9. The lift was measured on a symmetrical section with a 30 per cent chord flap, hinged in a manner similar to the flaps in this investigation. For flap displacements of 20° and less, about 98 per cent of the theoretical effect was attained.

The pitching characteristics and center of pressure movement are best studied by a consideration of the pitching moment taken about a point one-quarter of the chord behind the leading edge. The reason for taking the moment about this point is apparent from Munk's theory, which states that the moment about the one-quarter chord point is independent of the angle of attack and varies directly with the flap angle. Therefore, we may write

$$C_M=-m\delta \tag{3}$$

where the proportionality factor $m$ is independent of aspect ratio and may be found theoretically from Munk's integrals (References 4 and 5), or by Glauert's

method (Reference 6). Both methods give substantially the same result.

$$m=\frac{a_o}{\pi}(1-E)\sqrt{E(1-E)} \tag{4}$$

where $a_o$ is the slope of the lift curve for the airfoil of infinite aspect ratio. Experiment indicates (Reference 8) that for commonly used airfoils the value of $a_o$ is approximately 5.5 instead of $2\pi$, as the theory shows. Using 5.5 as the value of $a_o$, values of $m$ have been calculated for different values of $E$ and plotted against $E$ in Figure 24 for convenient reference. The theoretical straight lines with slope, $-m$, are drawn together with the experimental points in Figures 27 to 29. A study of these figures shows that for small flap displacements ($-10°$ to $+10°$) the actual and the theory agree closely. It might be added that this range covers most of the working range of control surfaces.

The torsional stresses at the hinge due to the air forces on the flap are of importance in the design of control surfaces. The hinge moment is best studied by a consideration of its relation to flap displacement and the lift. H. Glauert, in Reference 6, has theoretically derived an expression for the hinge moment coefficient ($C_h$), which is of the form

$$C_h=h_oC_L-h\delta \tag{5}$$

It is placed in this form because the parameters $h_o$ and $h$ are independent of aspect ratio. In brief, Glauert's method consists in assuming a distribution of vorticity of the form

$$kdx=cV[A_o(1+\cos\theta)+\sum_1^\infty A_n \sin n\theta \sin\theta]d\theta \tag{6}$$

where the first term gives the vorticity for a straight line airfoil and the coefficients of the sine series are dependent on the shape of the airfoil. By means of the process used in the above reference and noting the use of dynamic pressure, $\frac{1}{2}\rho V^2$, in place of the British usage, $\rho V^2$, the expressions for the parameters $h_o$ and $h$ are found to be

$$h_o=-\frac{1}{\pi E^2}\left[\left(\frac{3}{2}-E\right)\sqrt{E(1-E)}-\left(\frac{3}{2}-2E\right)\left(\frac{\pi}{2}-\cos^{-1}\sqrt{E}\right)\right] \tag{7}$$

$$h=\frac{4(1-E)\sqrt{E(1-E)}}{\pi E^2}\left[\frac{\pi}{2}-\cos^{-1}\sqrt{E}-\sqrt{E(1-E)}\right] \tag{8}$$

For ready reference, values of these parameters are plotted against $E$ in Figure 24. The parameter $h$ is the most interesting because it is the proportionality factor determining the variation in hinge moment with flap displacement. It will be noted that for values of $C_h$ plotted against $\delta$ at different lifts, the parameter $h$ is a measure of slope, hence straight lines having slopes equal to $h$ and representing the theoretical relationship for lifts corresponding to $C_L=0$, and $C_L=.6$ are drawn together with the experimental points in Figures 30 to 32.

A study of the above figures shows that the parameter $h$ affords a means of theoretically calculating the effect of flap displacement upon hinge moment coefficient which leads to results which agree closely with the actual. The parameter $h_o$, however, does not show such good agreement, due probably to a lack of precision in the measurement of the small forces encountered. The percentage error in $h_o$ appears high because the theoretical values of $h_o$ are very small. In other words, for flaps of small chord the hinge moment depends almost entirely on the flap displacement, being only slightly affected by the lift or attitude of the airfoil as a whole.

In order that these equations for the coefficients may be applied to airfoils not having symmetrical profiles, it is necessary to add a corrective constant to the right-hand side of Equations 1, 3, and 5. They will then take the form

$$C_L=a(\alpha-\alpha_o+k\delta) \tag{9}$$

$$C_M=-m\delta+C_{M_o} \tag{10}$$

$$C_h=h_o\,C_L-h\delta+C_{h_o} \tag{11}$$

The additional constants $\alpha_o$, $C_{M_o}$, and $C_{h_o}$ can be easily determined for any airfoil. $\alpha_o$ is the angle of zero lift of the undeformed section. $C_{M_o}$ is the pitching moment coefficient for the undeformed section and $C_{h_o}$ is the hinge moment coefficient for the undeformed section at zero lift.

## CONCLUSIONS

1. Downward displacement of a 10 or 20 per cent chord flap, on a R. A. F. 30 airfoil, to angles as large as 40° produces a progressive increase in the maximum normal force coefficient.

2. At Reynolds Numbers corresponding approximately to full scale for airplane wings the maximum normal force coefficient is higher than low-scale model tests would indicate for all downward flap displacements, but at the higher scale, displacing the flap does not produce as great a change in the maximum normal force coefficient.

3. The pitching moments and hinge moments obtained from these tests agree very well with the theoretical results for small flap displacements, regardless of the size of the flap.

4. For flaps 20 per cent of the chord or smaller the theory does not give a good measure of the actual flap effect on the lift. This is particularly true with the type of hinge used and at the higher values of the Reynolds Number.

5. The effect of flaps should be further investigated at large values of the Reynolds Number to find the effect of different types of hinges and fairings at the hinge, including also slots between the airfoil and the flap.

LANGLEY MEMORIAL AERONAUTICAL LABORATORY,
NATIONAL ADVISORY COMMITTEE FOR AERONAUTICS,
LANGLEY FIELD, VA., *April 2, 1930.*

## REFERENCES

1. Munk, Max M., and Miller, Elton W.: The Variable Density Wind Tunnel of the National Advisory Committee for Aeronautics. N. A. C. A. Technical Report No. 227 (1927).

2. Jacobs, Eastman N., Stack, John, and Pinkerton, Robert M.: Airfoil Pressure Distribution Investigation in the Variable Density Wind Tunnel. N. A. C. A. Technical Report No. 353 (1930).

3. ———: Aerodynamic Characteristics of Airfoils—IV. N. A. C. A. Technical Report No. 244 (1926).

4. Higgins, George J., and Jacobs, Eastman N.: The Effect of a Flap and Ailerons on the N. A. C. A.-M 6 Airfoil Section. N. A. C. A. Technical Report No. 260 (1927).

5. Munk, Max M.: The Determination of the Angles of Attack of Zero Lift and Zero Moment, Based on Munk's Integrals. N. A. C. A. Technical Note No. 122, (1923).

6. Glauert, H.: Theoretical Relationship for an Airfoil with hinged Flaps. Reports and Memoranda No. 1095 (1927).

7. ———: Airfoil and Airscrew Theory (1926).

8. Jacobs, Eastman N., and Anderson, Raymond F.: Large Scale Aerodynamic Characteristics of Airfoils as Tested in the Variable Density Wind Tunnel. N. A. C. A. Technical Report No. 352 (1929).

9. Smith, R. H.: Lift, Drag, and Elevator Hinge Moments of Handley-Page Control Surfaces. N. A. C. A. Technical Report No. 278 (1927).

10. Norton, F. H., and Brown, W. G.: The Pressure Distribution over the Horizontal Tail Surfaces of an Airplane—III. N. A. C. A. Technical Report No. 148 (1922).

# APPENDIX

## COMPUTATION OF WING LOAD CHARACTERISTICS BY MEANS OF THEORETICAL PARAMETERS FOR A WING WITH HINGED FLAP

In order to illustrate the use of the theoretical method, it has been felt desirable to give a numerical example using the theoretical parameters as a basis for monoplane wing load calculations. The lift, pitching moment (about the one-quarter chord point), and the hinge moment are computed for a symmetrical rectangular monoplane wing having a trailing edge flap. The dimensions of the wing and the conditions of flight are given below.

| | |
|---|---|
| Span | 50 feet. |
| Chord | 7 feet. |
| Flap chord | 1.4 feet (20 per cent chord). |
| Thickness | 12 per cent chord. |
| Incidence ($\alpha$) | 5°. |
| Flap angle ($\delta$) | 10° (.1745 radian). |
| Velocity | 100 m. p. h. |

**Calculation of the coefficients:**

The coefficients are computed by means of Equations 9, 10, and 11. The values of the 4 parameters ($k$, $m$, $h_\alpha$, and $h$) are read from the curves in Figure 24, and since the section is symmetrical, the constants $\alpha_0$, $C_{M_0}$, and $C_{h_0}$ are zero. The slope of the lift curve, $a$, is dependent upon aspect ratio and may be calculated by the method of Reference 8.

$$a=\frac{a_\alpha}{1+\frac{a_\alpha}{\pi R}(1+\tau)57.3}=.074 \text{ per degree} \qquad (12)$$

$$C_L=a(\alpha+k\delta).$$

From Figure 24 the value of $k$ is found to be 0.549, but experiment has shown this to be too high. Hence, the value used is computed from the high scale curves in Figure 26, the slope of the curves being equal to $a\,k$.

$$a\,k=.023 \text{ per degree}$$

$$k=\frac{.023}{.075}=.307$$

$$C_L=.074(5+.307\times 10)$$
$$=.598$$
$$C_M=-m\delta$$
$$=-.560\times .1745$$
$$=-.098$$

From this value of the moment coefficient the center of pressure may be found approximately by dividing by $C_L$.

$$C_p=\frac{C_M}{C_L}$$
$$=\frac{-.098}{.598}$$
$$=-.164$$

This represents the distance of the center of pressure measured as a fraction of the chord from the quarter-chord point. The negative sign indicates that it is behind this point.

$$C_h=h_\alpha C_L-h\delta$$
$$=-.080\times .598-.650\times .1745$$
$$=-.161$$

**Calculation of the Loads:**

The total loads are computed from the following equations in which $S$ is the area, $c$ is the chord, and $q$, the dynamic pressure.

$$q=\frac{1}{2}\rho V^2=\frac{1}{2}\times .00238\times\left(\frac{100\times 5280}{3600}\right)^2$$
$$=25.6 \text{ pounds per square foot.}$$
$$L=C_L\,q\,S$$
$$=.598\times 25.6\times 350$$
$$=5360 \text{ pounds.}$$
$$M=C_M\,q\,c\,S$$
$$=-.098\times 25.6\times 7\times 350$$
$$=-6150 \text{ pound-feet.}$$
$$M_h=C_h\,q\,c_f\,S_f$$
$$=-.161\times 25.6\times 1.4\times 70$$
$$=-404 \text{ pound-feet.}$$